Design and Synthesis of Substrate Analogue Inhibitors of Peptide Deformylase†

Thierry Meinnel,*,‡ Luc Patiny,§ Stéphane Ragusa,‡ and Sylvain Blanquet‡

Laboratoire de Biochimie and Département de Chimie et Synthèse Organique, UMR 7654 and 7652 Ecole Polytechnique, Centre National de la Recherche Scientifique, Ecole Polytechnique, F-91128 Palaiseau Cedex, France

Received November 4, 1998; Revised Manuscript Received January 8, 1999

ABSTRACT: Series of substrates derivatives of peptide deformylase were systematically synthesized and studied for their capacities to undergo hydrolysis. Data analysis indicated the requirement for a hydrophobic first side chain and for at least two main chain carbonyl groups in the substrate. For instance, Fo-Met-OCH_3 and Fo-Nle-OCH_3 were the minimal substrates of peptide deformylase obtained in this study, while positively charged Fo-Nle-$ArgNH_2$ was the most efficient substrate ($k_{cat}/K_m = 4.5 \times 10^5$ $M^{-1}\cdot s^{-1}$). On the basis of this knowledge, 3-mercapto-2-benzylpropanoylglycine (thiorphan), a known inhibitor of thermolysin, could be predicted and further shown to inhibit the deformylation reaction. The inhibition by this compound was competitive and proved to depend on the hydrophobicity at the P_1' position. Spectroscopic evidence that the sulfur group of thiorphan binds next to the active site metal ion on the enzyme could be obtained. Consequently, a small thiopseudopeptide derived from Fo-Nle-OCH_3 was designed and synthesized. This compound behaved as a competitive inhibitor of peptide deformylase with $K_I = 52 \pm 5$ μM. Introduction of a positive charge to this thiopeptide via addition of an arginine at P_2' improved the inhibition constant up to 2.5 ± 0.5 μM, a value 4 orders of magnitude smaller than that of the starting inhibitors. Evidence that this inhibitor, imino[(5-methoxy-5-oxo-4-[[2-(sulfanylmethyl)-hexanoyl]amino]pentyl)amino]methanamine, binds inside the active site cavity of peptide deformylase, while keeping intact the 3D fold of the protein, was provided by NMR. A fingerprint of the interaction of the inhibitor with the residues of the enzyme was obtained.

In eubacteria, the formylation of initiator methionyl-tRNAs by methionyl-$tRNA^{fMet}$ transformylase results in N-formylated nascent polypeptides (reviewed in ref *1*). The *N*-formyl groups are then removed by peptide deformylase (PDF,[1] EC 3.5.1.27), an essential enzyme in the bacterial kingdom (*2*, *3*). PDF activity was evidenced 30 years ago, but PDF proved to be so unstable that it could not be purified any further (*4*, *5*). The identification, cloning, and sequencing of the PDF gene (*fms* or *def*) in *Escherichia coli* revealed that the protein bears the HEXXH motif of the zinc metalloproteases superfamily (*3*, *6*−*8*). Purification to homogeneity of the overexpressed enzyme was achieved. Two forms could be separated at the last step of purification (*9*−*11*). Form I, which retains a firmly bound zinc ion, was first characterized but proved poorly active. Its 3D structure revealed a unique fold which, however, shares a secondary superstructure similar to that of other proteases displaying the HEXXH motif, such as thermolysin and metzincins (*12*−*14*). More recent work has indicated that the second form of PDF corresponds to the apoenzyme and that it derives from a very active but unstable enzyme associated to an extraordinarily labile divalent metal ion different from zinc (*10*, *15*, *16*). This form is believed to correspond to the physiologically active protein and the nature of the genuine ion was proposed to correspond to a ferrous ion (*15*−*17*). Interestingly, nickel can be exchanged with iron without any loss of specific activity. The nickel form is much more stable than the iron form, so that structural studies could be performed. The data revealed, however, no significant difference with respect to the zinc form (*12*, *18*).

The metal cation is tetracoordinated by one water molecule and by the side chains of the two histidines of the HEXXH motif and of a cysteine (*19*). The secondary structure scaffold and a complex network of hydrogen bonds in the active site enable the presentation to the metal of the sulfur group of that cysteine. Sequence comparisons, site-directed mutagenesis experiments, and biochemical characterization of several PDF originating from various microorganisms suggested the conservation of the 3D structure and catalytic mechanism for all bacterial PDF (*12*, *20*). The side chains thought to participate in the catalytic process are strictly conserved in the PDF family. Most of them belong to three signature

† L.P. was the recipient of a postdoctoral fellowship from the Ecole Polytechnique (Palaiseau, France). S.R. was the recipient of a scholarship from the French Ministère de l'Enseignement Supérieur et de la Recherche and the Institut de Formation Supérieure Biomédicale (Villejuif, France).

* Corresponding author. Tel 33 1 69 33 48 80. Fax 33 1 69 33 30 13. E-mail: titi@botrytis.polytechnique.fr.

‡ Laboratoire de Biochimie.

§ Département de Chimie et Synthèse Organique.

[1] Abbreviations: Fo, *N*-formyl; Nle, norleucine; PDF, peptide deformylase.

10.1021/bi982622r CCC: $18.00
Published on Web 03/16/1999

sequences: GXGLAAXQ, EGCLS, and QHEXDH (*12*, *20*). In addition, two carboxylate groups of the last two motifs make salt bridges with the guanidinium groups of an isolated but strictly conserved arginine.

Although many of the intimate features of PDF have been revealed for the past 5 years, the problem of substrate recognition and hydrolysis within the active site is still unsolved. In a previous work where NMR experiments could be carried out (*13*), the use of Fo-Met as a ligand showed that the chemical shifts of only a few NH of PDF in the vicinity of the metal were affected. This suggested that the *N*-formyl group was in the vicinity of the amide of the side chain of Gln50. However, because of slow hydrolysis of Fo-Met by PDF (*10*), finer experiments involving longer accumulation times could not be monitored. Clearly, to address the question of substrate recognition by PDF, a nonhydrolyzable molecule is required. To date, the only available analogues are product molecules of the reaction, such as Met-Ala-Ser. Nevertheless, the very weak binding constant of such ligands (50 mM) precludes their use in structural studies (*21*). The present study was initiated with the aim of designing more efficient substrate analogues.

MATERIALS AND METHODS

Peptide Deformylase Activity Measurements. E. coli peptide deformylase was purified as described (*10*). The standard peptide deformylase assay was coupled to formate dehydrogenase essentially as described in ref *21*. PDF activity was assayed at 37 °C as a function of time through the increase of the absorbance at 340 nm of NADH (ϵ_M = 6300 $M^{-1}\cdot cm^{-1}$). The standard assay was performed with 200 μL cells in a 1 cm optical path. The reaction mixtures contained 50 mM Hepes (pH 7.5), 1 mM Fo-Met-Ala (Bachem), 12 mM NAD^+ (Boehringer), 1 mM $NiCl_2$ and 4.5 units/mL yeast FDH (Sigma). The reaction was started by the addition of 5 μL of PDF diluted in 50 mM Hepes (pH 7.5), 1 mM $NiCl_2$, and 200 μg/mL bovine serum albumin (fraction V, Boehringer).

When a non-formyl group was removed from the substrate, the activity was measured by monitoring the unprotection of primary amines with the ninhydrin assay as previously reported (*9*, *19*). In this case, the deformylation reaction was usually carried out at 37 °C in an Eppendorff tube for varying times (0.5−120 min). The standard assay contained 50 mM Hepes (pH 7.5), 1 mM $NiCl_2$, and the indicated substrate. Each reaction (final volume of 50 μL) was triggered by the addition of purified PDF. The reaction was quenched by the addition of 0.5 mL of 5% trichloroacetic acid and chilled on ice. The tubes were centrifuged for 5 min, and 250 μL of the supernatants was collected to determine the concentration in primary amine (*22*).

NMR Spectroscopy. The NMR sample of the mixture of TNR and PDF was prepared in 20 mM perdeuterated Tris-HCl (pH 7.2) and 0.02% NaN_3 (w/v), in either $H_2O/^2H_2O$ (9:1 v/v) or 100% ^2H_2O. 2D and 3D NMR spectra were recorded at 318 K on a Bruker DRX600 spectrometer, using a doubly labeled 2 mM [^{13}C,^{15}N]Ni-PDF sample (*12*). 2D homonuclear and 3D heteronuclear experiments were recorded and processed as described previously (*12*, *13*).

Peptides, Peptide Derivatives, and Chemical Syntheses. Commercially available peptides were purchased from Bachem. The custom syntheses of Fo-Leu-Ala-Ser, Fo-Nva-Ala-Ser, Fo-Phe-Ala-Ser, Fo-Nle-Arg-NH_2, Fo-NleNH_2, Fo-Nle-$NHCH_3$, and Fo-Nle-Gly (Table 1) were made at Neosystem (98% purity). The other peptides were synthesized in the laboratory as follows. The substrates Fo-Met-(OCH_3) and Fo-Nle(OCH_3) were synthesized from the commercially available chlorohydrates and trimethyl orthoformate (*23*). Those esters were also reduced to the corresponding alcohols Fo-Metol and Fo-Nleol using sodium borohydride (*24*).

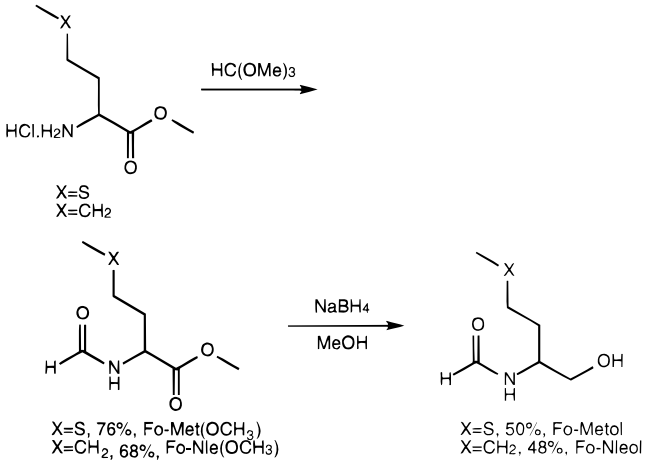

The substrate Fo-Met-Ala(OCH_3) was prepared using diazomethane starting from the commercially available formamide Fo-Met-Ala.

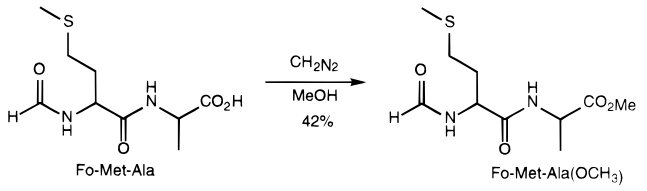

The thioformamides Tfo-Met and Tfo-Met(OCH_3) were synthesized from the corresponding amino acid with thiolformate **1** which was synthesized using a known procedure (*25*).

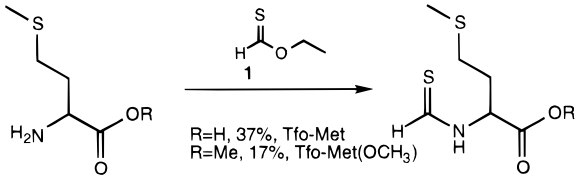

The inhibitor TN was readily available starting from the commercially available methyl hexanoate. In a first step the enolate reacts with formaldehyde in a poor yield to form the β-hydroxy ester **2**. This alcohol is then converted to the thiol using a Mitsunobu-like reaction. The use of thiolacetic

Scheme 1

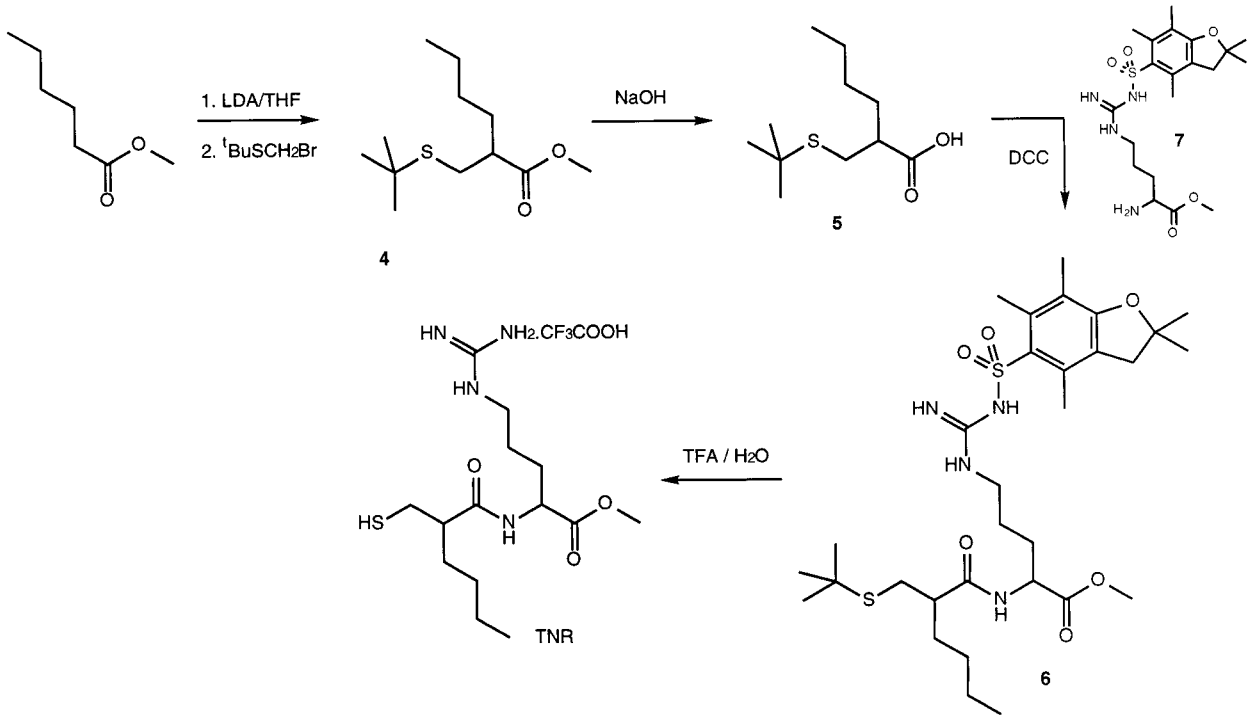

acid leads to the corresponding thioester **3** which can be methanolyzed to form the thiol TN (*26*).

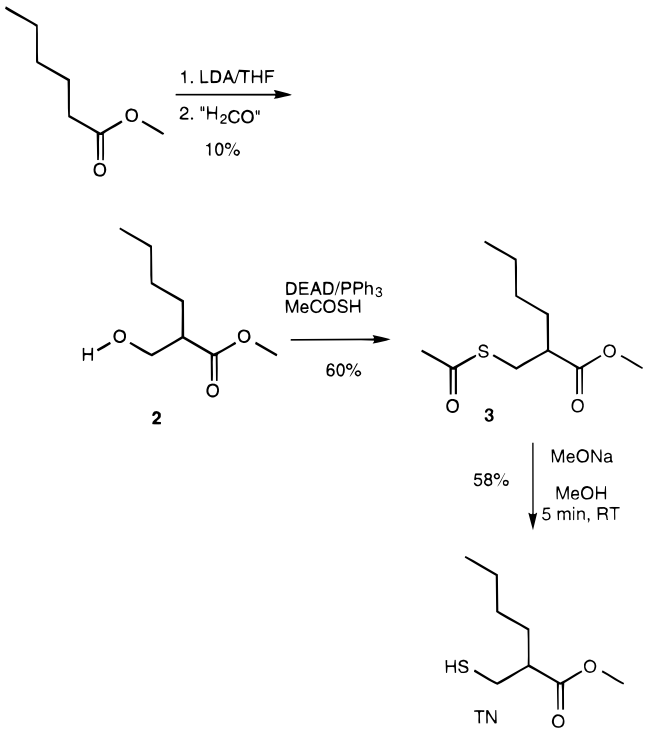

The inhibitor TNR was synthesized in four steps from methyl hexanoate. The reaction of the enolate with bromomethyl *tert*-butyl sulfide (*27*) produces to the ester **4**. This product was then hydrolyzed to give intermediate **5**. After coupling and deprotection, we were able to obtain the inhibitor TNR as a trifluoroacetate salt (*28*) (see Scheme 1).

TNR was finally purified by HPLC on a C18 5U column (32 × 150 mm; Alltech) in 0.1% trifluoroacetic acid buffer as follows. A 10−80% acetonitrile (Baker) gradient at a flow rate of 0.4 mL/min was performed for 60 min to elute the column.

The detailed procedure as well as the full characterization of the products is given as Supporting Information.

RESULTS

The Minimal Chemical Requirement for a Molecule To Be a Substrate of PDF. To identify the chemical functions supporting substrate recognition by PDF, we first attempted to synthesize the smallest possible substrate. Using *N*-Fo-Met-Ala-Ser or *N*-Fo-Nle-Ala-Ser as starting substrate peptides, we shortened the molecules to *N*-Fo-Met-Ala or *N*-Fo-Nle-Gly. Both exhibited similar deformylation efficiencies within a factor of 2 (Table 1). The substrate was then progressively trimmed from the carboxylate toward the *N*-formyl end. Compounds *N*-Fo-NleNH(CH_3), which is deprived of one carboxylate group compared to *N*-Fo-Nle-Gly, and *N*-Fo-NleNH_2, which further lacks one methyl group and the carboxylate, were nearly as good substrates as *N*-Fo-Met-Ala (Table 3). This strongly suggested that the chemical groups of the main chain at P_2' were not recognized by PDF. The catalytic efficiencies of deformylation of *N*-Fo-Nle or *N*-Fo-Met were also measured. They were reduced by 3 orders of magnitude as compared to *N*-Fo-Nle-Ala (Table 1). This result might indicate that the NH group at P′2 was crucial for catalysis and/or substrate recognition. However, we noticed that peptide derivatives with an acidic function were systematically less efficient substrates of PDF whatever the location of the acidic group in the peptide. For instance, two peptides with acidic groups at P_3' or P_4' (*N*-Fo-Met-Leu-Glu and *N*-Fo-Met-Ser-Asn-Glu) displayed significantly reduced deformylation efficiencies compared to the control and less acidic peptide (*N*-Fo-Met-Ala-Ser; Table 1). Consequently, the reduced deformylation efficiency of *N*-Fo-Nle compared to *N*-Fo-Nle(NH_2) might be caused by the

Table 1: Determination of the Chemical Functions That PDF Requires for a Molecule To Be Deformylated

peptide[a]	k_{cat} (s^{-1})[b]	K_m (mM)[b]	$k_{cat}/K_m \times 10^{-3}$ ($M^{-1}\cdot s^{-1}$)[b]	relative k_{cat}/K_m[d]
Fo-Met-Ala-Ser	210 ± 10	3.9 ± 0.6	54 ± 5	100
Fo-Met-Ser-Asn-Glu	180 ± 30	5.5 ± 1.8	32 ± 3	60
Fo-Met-Leu-Glu	47 ± 3	4 ± 1	12 ± 1	21
Fo-Ala-Ala-Ala	6 ± 1	52 ± 15	0.11 ± 0.01	0.20
Fo-Nle-Ala-Ser	220 ± 40	3.5 ± 1.1	62 ± 8	115
Fo-Leu-Ala-Ser	nm[e]	>15[e]	6 ± 2	11
Fo-Phe-Ala-Ser	100 ± 10	8 ± 1	13 ± 1	24
Fo-Nva-Ala-Ser	150 ± 20	10 ± 1	15 ± 2	28
Fo-Met-Ala(OCH_3)	360 ± 30	2.5 ± 0.4	140 ± 20	267
Fo-Nle-Arg-NH_2	290 ± 20	0.7 ± 0.1	450 ± 60	839
Fo-Met-Ala	230 ± 40	6.2 ± 1.5	37 ± 3	69
Fo-Nle-Gly	180 ± 20	5.4 ± 0.9	34 ± 4	63
Fo-Nle-NH(CH_3)	130 ± 20	12 ± 2	11 ± 1	20
Fo-Nle-NH_2	44 ± 6	7.5 ± 1.5	5.9 ± 0.6	11
Fo-Nle(OCH_3)	200 ± 20	6.3 ± 0.9	32 ± 2	59
Fo-Met(OCH_3)	180 ± 30	12.0 ± 2.8	15 ± 1	27
Fo-Metol	0.8 ± 0.2	24 ± 7	0.035 ± 0.002	0.06
Fo-Met	0.21 ± 0.02	2.5 ± 0.7	0.08 ± 0.01	0.16
Fo-Nle	0.12 ± 0.02	4.2 ± 1.4	0.03 ± 0.01	0.05
Tfo-Met(OCH_3)	>0.003[c]	>20[c]	0.0007 ± 0.0001	0.01[c]
Tfo-Met	>0.0007[c]	>20[c]	<0.0001[c]	<0.001
Fo-Asp	nm	nm	<0.00003	<0.00005
Fo-Gly	nm[c]	nm[c]	<0.00003[c]	<0.00005[c]

[a] Peptides were purchased from Neosystem or Bachem AG or synthesized as described in Materials and Methods. Metol means methioninol, i.e., a methionine with its carboxylate group replaced by methanol. Tfo means *N*-thioformyl. Nva, means norvaline (the side chain is *n*-propyl). nm means not measurable. [b] Initial velocities of deformylation were usually measured by using the formate dehydrogenase-coupled assay. The kinetic parameters were derived from iterative nonlinear least-squares fits of the Michaelis−Menten equation to the experimental values (*44*). Confidence limits on the fitted values were determined by 100 Monte Carlo simulations, using the experimental standard deviations on individual measurements. [c] Deformylation rates were measured with the ninhydrin assay. [d] A value of 100 was given to the k_{cat}/K_m value obtained with Fo-Met-Ala-Ser. [e] The low solubility of this peptide in water (<20 mM) prevented us from determining the catalytic parameters.

acidic character of the free C-terminal function. To test this possibility, *N*-Fo-Nle(OCH_3), with a methyl ester at the C-side, was synthesized. This molecule was as efficient a substrate of PDF as *N*-Fo-NleNH_2, the amide derivative. To ascertain that the relatively low catalytic efficiency of *N*-Fo-Nle as substrate was indeed caused by its acidic character, *N*-Fo-Met-Ala(CH_3) was synthesized and compared to *N*-Fo-Met-Ala. The neutral peptide was a much more efficient substrate than the acidic one (Table 1). At this stage, it should be noticed that *N*-Fo-Met-Ala(CH_3) was the best substrate for PDF we had ever assayed.

To assess the importance of the second carbonyl group of the substrate, *N*-Fo-Metol, with a hydroxyl instead of the C-terminal carboxylate, was synthesized. The associated k_{cat}/K_m was reduced by 3 orders of magnitude compared to the reference peptide, indicating thereby the role of the second carbonyl group in the reaction. To finally investigate whether the carbonyl function of the *N*-formyl group was important for catalysis, a thioformyl derivative, *N*-thioformyl-Met(CH_3), with the oxygen replaced by a sulfur, was synthesized. This molecule was not a substrate of PDF (Table 1).

From the above results, we concluded that (i) the binding to PDF of an acidic substrate is disfavored compared to that of a nonacidic one, (ii) the carbonyls of the two first peptide bonds are essential for catalysis, and (iii) the NH of the second amino acid in the substrate is not recognized by the enzyme. Actually, the absence of recognition of the second amide proton could be expected since *N*-Fo-Met-Pro-peptides, which are featured by the absence of such an amide proton, must be substrates of PDF in vivo.

Importance of the Hydrophobic Character of the First Side Chain. It was previously reported that the presence of a methionine side chain at P_1' in the substrate strongly contributed to the efficiency of hydrolysis by PDF (*10*). Accordingly, shortening of the chain to a single methyl led to a dramatic decrease of the deformylation rate (500-fold). However, substitution of the methionine side chain by that of norleucine (Nle; i.e., an *n*-butyl chain) had no consequence on the hydrolysis rate (Table 1). This indicated that the sulfur of methionine is not required for PDF action and that the hydrophobic character of the methionine side chain was enough to govern substrate recognition. We therefore studied the effects on enzyme activity of the substitution of the P′1 position of Fo-Met-Ala-Ser by other hydrophobic residues. The deformylation catalytic efficiencies of Fo-Nle-Ala-Ser, Fo-Leu-Ala-Ser, Fo-Nva-Ala-Ser (with Nva corresponding to norvaline, i.e. an unnatural amino acid with an *n*-propyl side chain), and Fo-Phe-Ala-Ser were measured. The k_{cat}/K_m values were nearly identical to those obtained with the control peptide (Fo-Met-Ala-Ser), within a factor of at most 9 (Table 1). This suggested the occurrence of a S′1 hydrophobic binding pocket in PDF, with little specificity for a given side chain. An *n*-butyl side chain at P′1 appeared, however, to be preferred.

A Positively Charged Group at P_2' and an Aromatic Ring at P_3' Strongly Improve the Affinity of a Peptide to PDF. Since all peptides displaying an acidic group were apparently badly recognized by PDF, we hypothesized that the introduction of a positive charge into a formylpeptide derivative might improve the affinity to PDF. To probe this idea, the deformylation of peptide Fo-Nle-Arg-NH_2 was studied. Remarkably, this peptide behaved as a particularly efficient substrate for PDF (Table 1), with a k_{cat}/K_m value improved by 12.2-fold compared to that of Fo-Met-Ala. Interestingly,

Table 2: Binding Constants of Several Peptide Derivatives to PDF

compound[a]	K_I (μM)[b]
NH_2-Met-Ala-Ser-OH	53 000 ± 9 000
NH_2-Phe-Gly-OH	>150 000
NH_2-Phe-Gly-NH_2	150 000 ± 50 000
NH_2-Phe-Arg-OH	18 000 ± 5 000
NH_2-Met-Arg-OH	3 800 ± 400
NH_2-Met-Arg-Phe-OH	370 ± 50
NH_2-Nle-Arg-Phe-NH_2	470 ± 50
NH_2-Met-Arg-Phe-Ala	400 ± 100
NH_2-Phe-Arg-βNA	95 ± 10
NH_2(Nle-OCH_3)	45 000 ± 10 000
OH-CH_2(Nle-OCH_3)	68 000 ± 7 000
S=CH(Nle-OCH_3)	>1 000
SH-$(CH_2)_2$-OH	>10 000[d]
SH-Ala-Pro-OH	>10 000[c]
SH-Phe-Gly-OH	189 ± 20
SH-CH_2(Nle-OCH_3) (TN)	52 ± 5
SH-CH_2-Nle-Arg-CH_3 (TNR)	2.5 ± 0.5

[a] Peptides were purchased from Neosystem or Bachem AG or synthesized as described in Materials and Methods. βNA means β-naphthylamide. [b] the deformylation rates were measured at 1 mM Fo-Met-Ala, a value much smaller than the K_m value (6.2 mM; Table 1) in the presence of various concentrations of each peptide derivative. Under those conditions, the plots of the inverse of the measured rate versus the concentration of the added compound yielded linear curves in all cases. This is perfectly in keeping with a competitive inhibition mechanism. Inhibition constants which correspond to dissociation constant were directly derived from the linear plots. [c] Not soluble above 2 mM and could not be assayed at a concentration higher than 1 mM. [d] Could not be assayed above 2 mM because it complexes nickel ions and precipitates in the optical cell.

this property was mostly caused by a decrease of the K_m value. To assess the effect of the arginine side chain, the inhibition constant of dipeptide Phe-Arg was compared to that of Phe-Gly and found was 8 times better (Table 2). Furthermore, the affinity of Met-Arg was measured and found to be 4 times as high as that of Phe-Arg, as expected from the respective behaviors of Fo-Met-Ala-Ser and Fo-Phe-Ala-Ser (Table 1).

It was recently reported that the introduction of a *p*-nitroanilide group in Fo-Met-Leu caused a decrease of the K_m value by 2 orders of magnitude, while the k_{cat} parameter was kept nearly unmodified (*11*). This strong effect was, however, unlikely to only result from the removal of the negative charge in the peptide since the catalytic efficiency of hydrolysis of Fo-Met-Ala(CH_3) by PDF was improved only 4 times compared to that of Fo-Met-Ala. This rather suggested that the addition of an aromatic ring at the C-end of a dipeptide could also bring supplementary affinity toward the protein. When an aromatic ring was added at P_3', we indeed noticed a 10-fold decrease of the binding constant to PDF (Met-Arg-Phe vs Met-Arg; Table 2). More remarkably, when a β-naphthylamide was added at the C-end of the same peptide, the dissociation constant was decreased by 200-fold (Phe-Arg compared to Phe-Arg-βNA; Table 2). Finally, the effect of the C-blocking of a formyltripeptide could be assessed through the study of the binding of peptides Nle-Arg-PheNH_2 and Met-Arg-Phe-Ala. The corresponding binding constants were near identical compared to that of the control peptide (Nle-Arg-PheNH_2; Table 2).

From the above results, we concluded that the combination of a hydrophobic side chain at P_1', a basic side chain at P′2, and a C-terminal hydrophobic blocking group gave an *N*-formyl peptide the highest affinity to PDF, with potential increases of the association constant by 2−3 orders of magnitude.

Design of a Substrate Analogue of PDF. The resemblance between the active sites of PDF, thermolysins, and metzincins (*12*, *13*) can be used to design a substrate analogue capable of resisting hydrolysis by PDF. Thiol, phosphonate, sulfodiimide, carboxylate, or hydroxamate groups have been already introduced at the scissile bond of the substrates of thermolysin and metzincins (*29*, *30*). In many cases, the resulting peptide derivatives displaying strong inhibitory potencies were obtained (*31*−*39*). In the course of the design of substrates analogues of PDF, the substitution of such groups for the *N*-formyl appeared therefore very promising.

Because of the aforementioned, repulsion between PDF and substrates by negative charges, phosphate, or carboxylate groups were discarded a priori. By assuming that the potency of an inhibitor is governed by the strength of its coordination to the metal (*31*), the thiol derivatives, which are known to make tight complexes with nickel or ferrous ions, appeared most attractive to us. Note, however, that 2-mercaptoethanol up to 10 mM did not inhibit PDF activity (Table 2; Figure 1A). To fit a thiol extremity next to the nickel ion of PDF, we imposed that the structure of the putative analogue closely resemble that of the best substrate of PDF. To achieve this, the minimal requirements were the occurrence of a side chain displaying a hydrophobic character at P′1 and that of a carbonyl group. In this context, it was striking that the chemical structure of 3-mercapto-2-benzylpropanoylglycine, a commercially available molecule known as thiorphan, satisfied these requirements. Accordingly, we found that it was a competitive inhibitor of PDF (K_I = 189 ± 40 μM; Figure 1).

Captopril (3-mercapto-2-methylpropanoylproline) also inhibited PDF activity. Nevertheless, the associated K_I was 2 orders of magnitude higher than that of thiorphan (Table 2). The main difference between captopril and thiorphan is at the level of the nature of the first side chain (a methyl instead of a phenyl). We concluded, therefore, that the phenyl group of thiorphan directly participated in the binding to PDF through recognition by the S_1' binding pocket. In addition, peptides Phe-Gly (same as thiorphan but with the CH_2SH replaced by NH_2) and Phe-GlyNH_2 behaved as weak inhibitors of PDF, therefore indicating a direct participation of the thiol group in the stabilization of the complex. When peptide deformylase was saturated with thiorphan, two additional absorbance maxima, at 317 and 403 nm, respectively, were observed in the electronic spectrum of PDF (Figure 2A,B). This feature is strong evidence in favor of a charge transfer from the nickel of PDF to the sulfur of thiorphan. Such sulfur to metal charge transfer was already noticed in the case of cobalt-substituted thermolysin incubated with analogous thiol-containing substrate analogues (*40*). Upon titration of PDF by thiorphan, the intensity of the absorbance at both 317 and 403 nm increased in a hyperbolic manner (Figure 2C). A binding constant of 178 ± 20 μM was deduced from this experiment, in keeping with the K_I value deduced from the inhibition study (189 ± 40 μM, see above). When compared to that of Zn-PDF, the electronic spectrum of Ni-PDF is characterized by an additional absorbance maximum at 350 nm. This peak was interpreted as resulting from a charge transfer from nickel to the sulfur of the metal-coordinating cysteine, Cys90 (*10*), a feature indicative of the

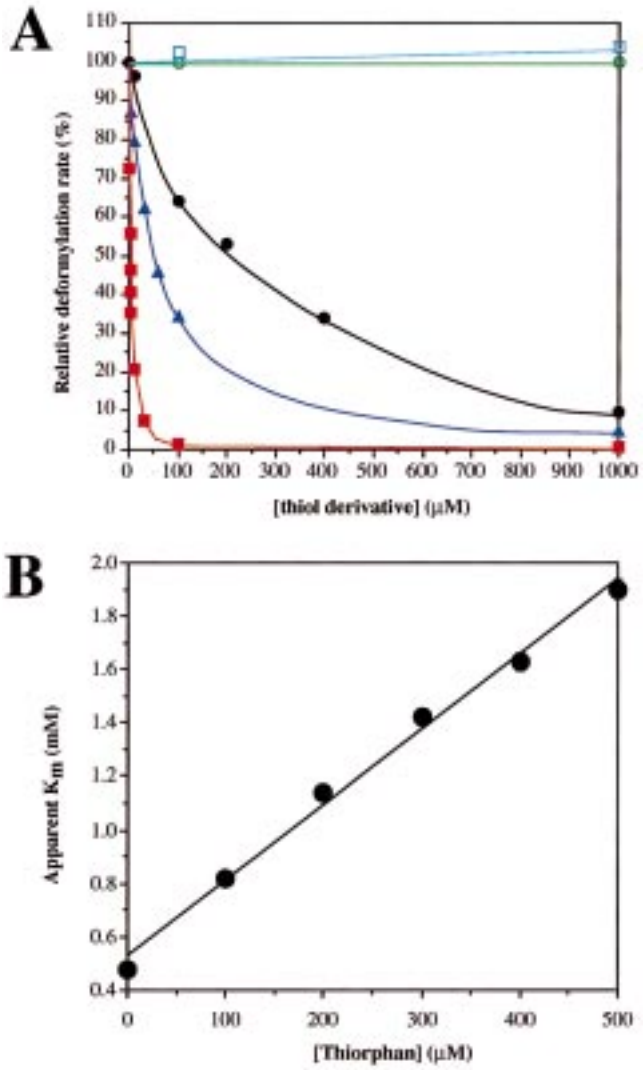

FIGURE 1: Thiol derivatives are competitive inhibitors of PDF. Panel A: Kinetics of deformylation were performed in the presence of 1 mM Fo-Met-Ala and of increasing concentrations in 2-mercaptoethanol (green open circles), captopril (light blue open squares), thiorphan (black circles), TN (dark blue triangles), or TNR (red squares). Relative deformylation rates are plotted as a function of the compound concentrations. A rate value of 100 corresponds to 32 s^{-1}. Panel B: Kinetics of deformylation were performed using varying concentrations in Fo-Nle-ArgNH_2 as the substrate and increasing amounts of thiorphan. k_{cat} and K_m values were derived from iterative nonlinear least-squares fits of the Michaelis−Menten equation to the experimental value (*44*). Confidence limits on the fitted values were determined by 100 Monte Carlo simulations, using the experimental standard deviations on individual measurements. The catalytic constant was not modified within the standard error, a behavior which is indicative of a competitive scheme. The apparent K_m value is plotted as a function of the concentration in thiorphan. In a competitive scheme, the slope is proportional to the K_I value.

vicinity of the sulfur group of this ligand and of the nickel ion. We noticed that the intensity of the maximum at 350 nm of PDF remained unaffected upon binding of thiorphan (Figure 2B). This suggested that the sulfur of Cys90 was not displaced by the sulfur of thiorphan. Finally, since the thiol group in thiorphan accounted for a significant part of the affinity to PDF, we concluded that an ionic interaction between the sulfur group and nickel participated in the stabilization of the thiorphan−PDF complex. Most likely,

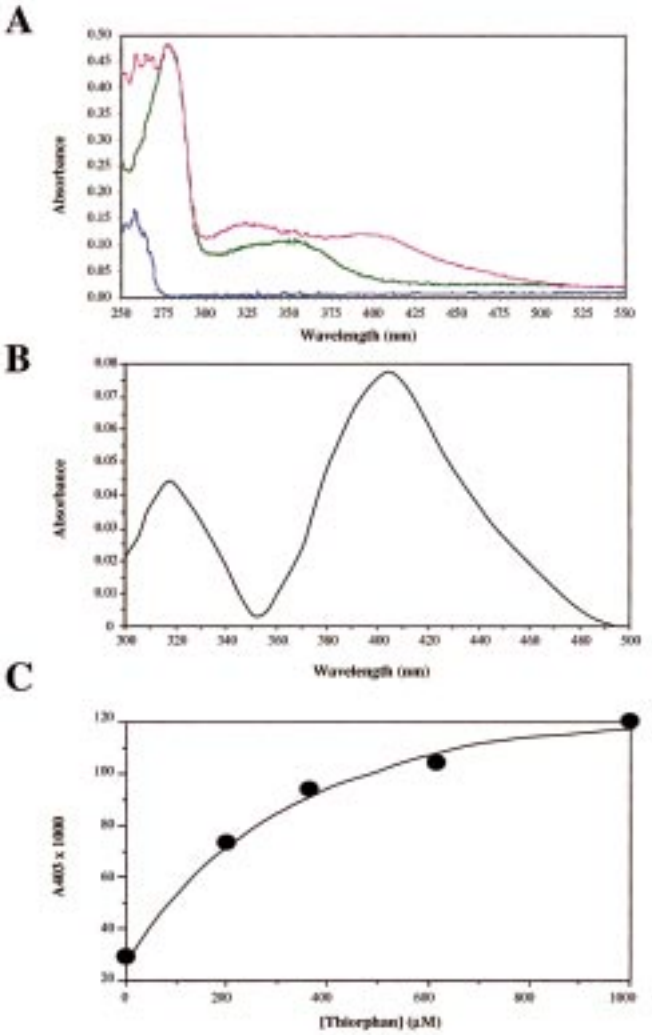

FIGURE 2: Charge transfer of the catalytic nickel to the sulfur of thiorphan. Panel A: The electronic spectra of 1 mM thiorphan (blue), 0.2 mM PDF (green), and a mixture of both (pink) were performed in 50 mM Hepes (pH 7.5) with a UV2101-PC spectrophotometer (Shimadzu). The spectrum of 1 mM thiorphan plus 0.2 mM $NiCl_2$ was identical to that of thiorphan alone. Panel B: The characteristic electronic spectrum resulting from the binding of thiorphan to PDF is shown. It was calculated as follows: the absorbance value of the mixture of both thiorphan and PDF measured at a given wavelength (see the experiment shown in panel A) minus the sum of the absorbances of thiorphan and PDF measured separately. Panel C: A PDF sample (0.2 mM) was mixed with increasing concentrations in thiorphan and the resulting absorbance measured at 403 nm. A saturation curve is shown.

thiorphan ligates the missing valence of nickel by exchange with a water molecule.

Synthesis of an Efficient Substrate Analogue of PDF. Thiorphan displays a phenyl group at P_1', whereas, as shown in Table 2, an *n*-butyl appears to be preferred by PDF at this position. In addition, the C-terminus of thiorphan is unblocked. We therefore chose to substitute a thiol for the *N*-formyl group of the shortest efficient substrate of PDF, Fo-Nle-OCH_3 (Table 1). The thiol derivative corresponding to this molecule (TN) could be synthesized. TN exhibited a strong competitive inhibitory capacity of PDF activity. The associated inhibition constant (52 ± 12 μM) was 4-fold lower than that measured with thiorphan. If the sulfur group of TN was replaced by either a hydroxyl, a thioformyl, or an amino group, the inhibition constant always rose by at least

Table 3: Main Changes of PDF Chemical Shifts Observed upon Binding of TNR

atom	$\Delta\delta$ ^{15}N or ^{13}C (ppm)[b]	atom	$\Delta\delta$ ^{1}H (ppm)[c]
C90 *C*A	+7.2	C90 *H*A	+1.32
Q50 *N*E	−5.5	Q50 *H*NE1	+0.92
L91 *N*H	−4.5	L91 *H*N	+0.83
V59 *N*H	+3.0	G89 *H*N	+0.57
I86 *N*H	+2.0	H7 *H*N	−0.57
I44 *N*H	+1.5	Q50 *H*NE2	+0.51
G45 *N*H	−1.5	G43 *H*A1	+0.45
A47 *N*H	+1.5	E41 *H*N	+0.40
		G45 *H*N	+0.35
		C90 *H*N	−0.34
		G43 *H*N	−0.31

[a] The complete set of ^{13}C, ^{15}N, and ^{1}H resonances of PDF mixed with TNR (1:2 molar ratio) was assigned and compared to that of the unbound protein sample (BioMagRes Bank accession number 4089 and ref *12*). Each chemical shift value obtained in the bound state was subtracted from the value in the unbound state. The main changes are listed and ordered from the greatest to the smallest. [b] Only changes greater than 1.0 ppm are reported. [c] Only changes greater than 0.25 ppm are reported.

2 orders of magnitude (Figure 1A; Table 2). Consequently, as expected from the behavior of thiorphan, the sulfur group of TN plays a crucial role in the binding free energy to PDF.

From the above results and given the positive effect of the addition of an arginine at P_2' on the affinity of a peptide to PDF, we expected that the thiol derivative of Nle-Arg-OCH_3 (called TNR) would exhibit a binding constant to PDF markedly improved compared to that of thiorphan or TN. TNR was therefore synthesized and its binding constant for PDF determined from inhibition experiments. Remarkably, the TNR inhibition constant was 21-fold better than that of TN ($K_I = 2.5 \pm 0.5$ μM; Figure 1A; Table 2). Furthermore, compared to thiorphan and TN, TNR displayed a high solubility in water, most likely due to the hydrophilicity brought by the arginine side chain.

NMR Study of the Interaction between PDF and TNR. In an attempt to get further information on the specificity of the interaction between TNR and PDF, an NMR analysis of a 1:2 (molar ratio) ^{13}C/^{15}N PDF/unlabeled TNR mixture was performed. First, it was noticed that, upon mixing the protein and the inhibitor, the chemical shifts of some protons of the inhibitor were clearly affected, with broadening and shifting of a few well-defined peaks as evidenced after ^{12}C filtering of the 1D spectrum of the mixture (data not shown). This behavior was demonstrative of the formation of a complex between the two molecules.

A nearly complete assignment of the ^{1}H, ^{13}C, and ^{15}N resonances of the protein could then be obtained using experimental conditions (2 mM PDF, 318 K, pH 7.2) identical to those used with the free enzyme (*12*). Interestingly, the comparison between the two data sets indicated that, while the majority (i.e., more than 1500) of the chemical shifts were left unmodified, a small subset (i.e., less than 20) showed significant change (Table 3). Among them, the chemical shifts corresponding to the amino group of the side chain of Gln50, the CHα of Cys90, and the amide groups of Leu91 and Gly45 were the most affected (Table 3). Such modification of the chemical environment of these residues was most probably due to a donor or acceptor group of the ligand. The occurrence of a charge transfer from the nickel

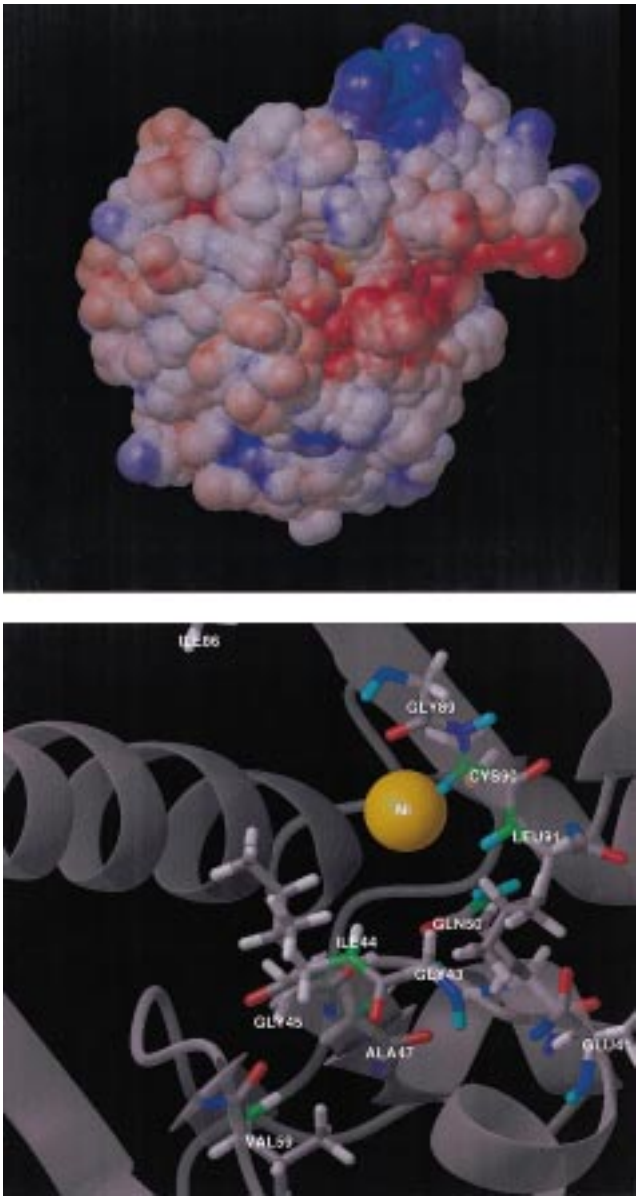

FIGURE 3: Protein cartoon of the molecular surface of PDF. The figure was prepared with the help of the MOLMOL software (*45*) using the coordinates of the crystallographic model of the full-length protein (*14*). Negatively and positively charged regions are colored in red and blue, respectively. The metal ion is shown as a yellow sphere. Panel A (top): The electrostatic potential of the side of PDF corresponding to the entry of the active site of PDF is shown. Panel B (bottom): Close-up of the previous view. The residues exhibiting a strong change of one of their chemical shifts upon binding of TNR according to the NMR analysis (Table 3) are displayed and labeled. The atoms undergoing such displacement of their chemical shifts are colored in green (C and N) or cyan (H).

of the protein to the sulfur of thiorphan (Figure 2) or TNR (data not shown) indicated close vicinity of the metal and of the sulfur group. Since the amino group of the Gln50 side chain, the CHα of Cys90, the amide group of Leu91, and the metal lie within a 4 Å radius sphere in the 3D structure of the free enzyme, it was likely that the sulfur group of TNR was responsible for the chemical shifts observed. Regarding the remainder of the chemical shifts undergoing strong displacement (Table 3), we noticed that they all were clustered next to the active site cavity (Figure 3). The inhibitor appeared, therefore, highly specific for the catalytic

site of PDF and mimicked the substrate, as expected. The fingerprint of the interaction of TNR with PDF is shown in Figure 3B.

In addition to the above assignment, the nearly complete set of protein−protein NOEs, including all of those characteristic for the secondary structure, was redetermined. It was found to not have been modified by the presence of the ligand. This established that the 3D structure of the protein was insensitive to the binding of TNR and that the inhibition of PDF activity by this ligand resulted only from the occupation of the active site, and not from a structure modification.

DISCUSSION

Here, we first show that PDF recognizes only the HCO-NH-CH(P′1)-CO groups of a molecule, with P′1 likely corresponding to a hydrophobic side chain. For instance, Fo-Nle-OCH_3 is the simplest substrate that PDF can efficiently hydrolyze. Therefore, PDF works as an extremely simplified aminopeptidase, with no S1 or S_2' subsites but with a true S_1' site. We also report that the length of a peptide substrate can be extended and that negatively charged peptides should be avoided. Electrostatic repulsion between the significantly negatively charged local electrostatic potential of the active site of PDF and the substrate molecules is likely to explain this behavior (Figure 3A). In this context, according to the present work, it is interesting that Fo-Met-$tRNA^{fMet}$, the tRNA molecule required in translation initiation, contains a priori all of the chemical groups required for the deformylation occurring. However, this molecule was shown not to be a substrate of PDF (*5*). It is therefore tempting to speculate that the negative charges borne by the phosphates of the tRNA participate in preventing its binding to PDF.

In this report, we could synthesize progressively and rationally a thiopeptide derivative (TNR) which specifically inhibits PDF activity by mimicking the substrate. It exhibits a binding constant in the micromolar range. It should be stressed that the binding strength of this substrate analogue has been improved by 4 orders of magnitude with respect to the starting molecule (Met-Ala-Ser). Such dissociation constant appears now low enough to undertake a structural analysis of the TNR−enzyme complex and to gain further information about the structure of a PDF−substrate complex. Besides the fundamental question of substrate−PDF recognition at the 3D level, the design and optimization of inhibitors have obvious relevance in the field of anti-biotherapy. In bacterial protein synthesis, peptide deformylase appears particularly well suited for the discovery of new antibacterial agents. This enzyme is indeed unique to eubacteria, it is an essential activity for cell growth, its 3D fold is very well conserved in the bacterial world, and the conditions of an easy assay of its activity have been recently set (*2*, *3*, *20*, *21*).

In the war against pathogenic bacteria, with respect to the traditional but nowadays noninnovating screenings for bacterial cell growth inhibitory agents, rational drug design is now considered as the optimal way to find new molecules (*41*). Usually, having selected a target, high-throughput screenings of libraries made of hundreds of thousands of uncharacterized natural compounds are performed (*42*), hits selected, and leads defined. Alternatively, and more rationally again, an optimized knowledge of the catalytic mechanism together with the help of the 3D structure of the target may be used to design such molecules de novo (*43*), by-passing thereby high-throughput screenings of random products. In this context, our work sheds light on what such a "lead" of PDF inhibitors could resemble to. Although the binding strength of TNR to PDF appears yet insufficient for this molecule to be already used as an antibiotic, it provides promising bases for a future design of such a drug, using TNR as the lead. As suggested in this paper (Table 2), the replacement of the OCH_3 at the C-terminus of TNR by a β-naphthylamide, for instance, could further improve the binding constant by 2 orders of magnitude.

ACKNOWLEDGMENT

We thank J.-Y. Lallemand for encouragement and interest, F. Dardel for help with the NMR spectroscopy and many stimulating discussions throughout this work, and P. Plateau for critical reading of the manuscript.

SUPPORTING INFORMATION AVAILABLE

The detailed procedure of the various chemical syntheses described in Materials and Methods as well as the full characterization of the products. This material is available free of charge via the Internet at http://pubs.acs.org.

REFERENCES

1. Meinnel, T., Mechulam, Y., and Blanquet, S. (1993) *Biochimie 75*, 1061−1075.
2. Meinnel, T., and Blanquet, S. (1994) *J. Bacteriol. 176*, 7387−7390.
3. Mazel, D., Pochet, S., and Marlière, P. (1994) *EMBO J. 13*, 914−923.
4. Adams, J. M. (1968) *J. Mol. Biol. 33*, 571−589.
5. Livingston, D. M., and Leder, P. (1969) *Biochemistry 8*, 435−443.
6. Meinnel, T., Guillon, J.-M., Mechulam, Y., and Blanquet, S. (1993) *J. Bacteriol. 175*, 993−1000.
7. Guillon, J.-M., Mechulam, Y., Schmitter, J.-M., Blanquet, S., and Fayat, G. (1992) *J. Bacteriol. 174*, 4294−4301.
8. Meinnel, T., and Blanquet, S. (1993) *J. Bacteriol. 175*, 7737−7740.
9. Meinnel, T., and Blanquet, S. (1995) *J. Bacteriol. 177*, 1883−1887.
10. Ragusa, S., Blanquet, S., and Meinnel, T. (1998) *J. Mol. Biol. 280*, 515−523.
11. Rajagopalan, P. T. R., Datta, A., and Pei, D. (1997) *Biochemistry 36*, 13910−13918.
12. Dardel, F., Ragusa, S., Lazennec, C., Blanquet, S., and Meinnel, T. (1998) *J. Mol. Biol. 280*, 501−513.
13. Meinnel, T., Blanquet, S., and Dardel, F. (1996) *J. Mol. Biol. 262*, 375−386.
14. Chan, M. K., Gong, W., Rajagopalan, P. T. R., Tsai, C. M., and Pei, D. (1997) *Biochemistry 36*, 13904−13909.
15. Rajagopalan, P. T. R., Yu, X. C., and Pei, D. (1997) *J. Am. Chem. Soc. 119*, 12418−12419.
16. Groche, D., Becker, A., Schlichting, I., Kabsch, W., Schultz, S., and Wagner, A. F. V. (1998) *Biochem. Biophys. Res. Commun. 246*, 342−346.
17. Rajagopalan, P. T. R., and Pei, D. (1998) *J. Biol. Chem. 273*, 22305−22310.
18. Becker, A., Schlichting, I., Kabsch, W., Schultz, S., and Wagner, A. F. V. (1998) *J. Biol. Chem. 273*, 11413−11416.
19. Meinnel, T., Lazennec, C., and Blanquet, S. (1995) *J. Mol. Biol. 254*, 175−183.

20. Meinnel, T., Lazennec, C., Villoing, S., and Blanquet, S. (1997) *J. Mol. Biol. 267*, 749−761.
21. Lazennec, C., and Meinnel, T. (1997) *Anal. Biochem. 244*, 180−182.
22. Moore, S., and Stein, W. H. (1954) *J. Biol. Chem. 211*, 907−913.
23. Kozlowski, M. C., and Bartlett, P. A. (1996) *J. Org. Chem. 22*, 7681−7696.
24. Itov, Z. I., L'vova, S. D., Gunar, V. I., and Bekker, A. R. (1977) *Pharmacol. Chem. J. 11*, 646−649.
25. Stowell, J. C., Ham, B. M., Esslinger, M. A., and Duplantier, A. J. (1989) *J. Org. Chem. 54*, 1212−1213.
26. Gennari, C., Molinari, F., Piarulli, U., and Bartoletti, M. (1990) *Tetrahedron 46*, 7289−7300.
27. Bashiardes, G., and Davies, S. G. (1987) *Tetrahedron Lett. 45*, 5563−5564.
28. Carpino, L. A., Shroff, H., Triolo, S. A., Mansour, E. M. E., Wenschuh, H., and Albericio, F. (1993) *Tetrahedron Lett. 49*, 7829−7832.
29. Cushman, D. W., Cheung, H. S., Sabo, E. F., and Ondetti, M. A. (1977) *Biochemistry 16*, 5484−5491.
30. Nishino, N., and Powers, J. C. (1979) *Biochemistry 18*, 4340−4347.
31. Browner, M. F., Smith, W. W., and Castelhano, A. L. (1995) *Biochemistry 34*, 6602−6610.
32. Bode, W., Reisemer, P., Huber, R., Kleine, T., Schnierer, S., and Tschesche, H. (1994) *EMBO J. 13*, 1263−1269.
33. Stams, T., Spurlino, J. C., Smith, D. L., Wahl, R. C., Ho, T. F., Walid Qoronfleh, M., Banks, T. M., and Rubin, B. (1994) *Nat. Struct. Biol. 1*, 119−123.
34. Gooley, P. R., O'Connell, J. F., Marcy, A. I., Cuca, G. C., Salowe, S. P., Bush, B. L., Hermes, J. D., Esser, C. K., Hagmann, W. K., Springer, J. P., and Johnson, B. A. (1994) *Nat., Struct. Biol. 1*, 111−118.
35. Cirilli, M., Gallina, C., Gavuzzo, E., Giordano, C., Gomis-Rüth, F. X., Gorini, B., Kress, L. F., Mazza, F., Paglialunga Paradisi, M., Pochetti, G., and Politi, V. (1997) *FEBS Lett. 418*, 319−322.
36. Borkakoti, N., Winkler, F. K., Williams, D. H., D′Arcy, A., Broadhurst, M. J., Brown, P. A., Johnson, W. H., and Murray, E. J. (1994) *Nat. Struct. Biol. 1*, 106−110.
37. Grams, F., Reinemer, P., Powers, J. C., Kleine, T., Pieper, M., Tschesche, H., Huber, R., and Bode, W. (1995) *Eur. J. Biochem. 228*, 830−841.
38. Grams, F., Dive, V., Yiotakis, A., Yiallouros, A., Vassiliou, S., Zwilling, R., Bode, W., and Stöcker, W. (1996) *Nat. Struct. Biol. 3*, 671−675.
39. Matthews, B. W. (1988) *Acc. Chem. Res. 21*, 333−340.
40. Holmquist, B., and Vallee, B. L. (1979) *Proc. Natl. Acad. Sci. U.S.A. 76*, 6216−6220.
41. Meinnel, T. (1999) *Pathol. Biol.* (in press).
42. Broach, J. R., and Thorner, J. R. (1996) *Nature 384* (Suppl.), 14−16.
43. Blundell, T. (1996) *Nature 384* (Suppl.), 23−26.
44. Dardel, F. (1994) *Comput. Appl. Biosci. 10*, 273−275.
45. Koradi, R., Billeter, M., and Wüthrich, K. (1996) *J. Mol. Graphics 14*, 51−55.

BI982622R